Appl Phys B (2010) 99: 769–773
DOI 10.1007/s00340-010-3960-7

Applied Physics B
Lasers and Optics

Red and near infrared down-conversion in Er^{3+}/Yb^{3+} co-doped YF_3 performed by quantum cutting

S. Xiao · X. Yang · J.W. Ding

Received: 26 October 2009 / Revised version: 24 January 2010 / Published online: 16 March 2010

Abstract Er^{3+}/Yb^{3+} co-doped YF_3 powder is prepared by combining a nitrate decomposition method with a NH_4HF_2 fluorization process, from which efficient energy transfer induced down-conversion is achieved. An absorbed 365 nm near ultraviolet photon is split into two photons of 650 nm red and 1000 nm near infrared radiations, both falling in the responding region of Si-based solar cells. The quantum cutting mechanism has been proposed and discussed and the energy transfer efficiency for the quantum cutting is evaluated by developing an emission intensity ratio contrast method. The investigation might offer a new possible approach to achieve Si-based solar cells of high efficiency by down-converting the near ultraviolet part of the solar spectrum.

Quantum cutting (QC) was firstly reported in Pr^{3+} doped YF_3 and $NaYF_4$ phosphors in the early 1970s [1, 2]. It could generate two low-energy photons from an absorbed incident high energy photon, by which the necessary redshift of the absorbed radiation is obtained without losing energy efficiency. This is considered as an exciting scenario toward the development of superior luminescent materials and devices [1–4]. After that, QC has also been witnessed in other materials doped with a single rare earth ion such as Pr^{3+}, Tm^{3+} and Gd^{3+} [3, 4].

The QC down-conversion based on an ion-couple was firstly reported in $LiGdF_4$ phosphor by Wegh [5], of which a vacuum ultraviolet photon is absorbed by Gd^{3+} and two red photons are then emitted by Eu^{3+} ions. Thereafter, many people attached great importance to QC by the combination of two or even three ions such as $Er^{3+} \rightarrow Gd^{3+}$ [6], $Gd^{3+} \rightarrow Tb^{3+}$ [7], $Pr^{3+} \rightarrow Mn^{2+}$ [8], $Pr^{3+} \rightarrow Cr^{3+}$ [9] and $Er^{3+} \rightarrow Gd^{3+} \rightarrow Tb^{3+}$ [10]. In these cases, the absorbed energy of the donor ions is transferred stepwise to the acceptor ions, and two photons of low energy are obtained. These QC phosphors can enhance luminescence emission in the visible region and have important applications in more efficient plasma display panels and mercury-free fluorescent tubes.

Recently, near infrared QC performed by cooperative energy transfers has been reported, which is also based on the combination of two ions [11–14]. In Tb^{3+} and Yb^{3+} co-doped YPO_4 [11], for instance, a cooperative energy transfer from Tb^{3+} to two Yb^{3+} ions leads to the photon doubling in the near infrared region. Similar phenomena have also been observed in several other rare earth coupled systems such as Pr^{3+}/Yb^{3+} [12], Tm^{3+}/Yb^{3+} [12, 13] and Ce^{3+}/Yb^{3+} [14] co-doped crystals or glasses. These phosphors can convert 484, 489, 475, and 330 nm photons into doubled 1000 nm photons, respectively. Since the energy of the converted photons is just above the band edge of crystalline Si, the energy losses by thermalization of electron hole pairs are minimized. Therefore, near infrared QC induced by cooperative energy transfer can enhance the energy efficiency of silicon-based solar cells in theory, which has attracted intense attention.

S. Xiao (✉) · X. Yang · J.W. Ding
Institute for Nanophysics and Rare-earth Luminescence,
Xiangtan University, Xiangtan 411105, China
e-mail: xiaosiguo@xtu.edu.cn
Fax: +86-731-58292468

X. Yang · J.W. Ding
Key Laboratory of Low Dimensional Materials & Application
Technology, Xiangtan University, Xiangtan, Hunan 411105,
P.R. China

J.W. Ding
e-mail: jwding@xtu.edu.cn

The Er^{3+}/Yb^{3+} couple has been recognized as one of the most efficient systems for obtaining frequency upconversion because of the effective energy transfer from Yb^{3+} to Er^{3+} [15]. According to the Förster–Dexter theory [16], however, there are also several possible pathways for the energy transfer from Er^{3+} to Yb^{3+}, due to the abundant levels of Er^{3+}. Moreover, the Er^{3+} ion has strong absorption in the near ultraviolet. Thus the Er^{3+}/Yb^{3+} couple might also be a potential system to down-convert the near ultraviolet photon into doubled photons of low energy, meeting the requirement of the Si-based solar cells.

In this paper, Er^{3+}/Yb^{3+} co-doped YF_3 powder is newly prepared by combining a nitrate decomposition method with a NH_4HF_2 fluorization process [17], and the properties of down-conversion are explored. Due to the energy transfer between the coupled ions, an efficient down-conversion is observed. Different from the previously reported cooperative energy transfer down-conversion [12–14], a cross-relaxation energy transfer in the Er^{3+}/Yb^{3+} co-doped YF_3 splits an absorbed 365 nm near ultraviolet photon into two photons of 650 nm red and 1000 nm near infrared radiations, both of them falling in the responding region of Si-based solar cells. This shows that the cross-relaxation energy transfer-induced QC can also satisfy the absorption of Si, providing a new photon down-conversion method in enhancing the Si-based solar cells. A mechanism of the QC has been proposed and further discussed. By contrasting the 365 and 488 nm excited emission intensity ratios, the energy transfer efficiency for QC is evaluated.

To obtain the Yb^{3+}, Er^{3+} co-doped YF_3 sample, first an aqueous solution containing $Y(NO_3)_3$ (purity of 99.99%), $Er(NO_3)_3$ (purity of 99.99%), and $Yb(NO_3)_3$ (purity of 99.99%) was dried at 80°C and then decomposed at 500°C to obtain the Yb^{3+} and Er^{3+} co-doped Y_2O_3 powder. Then the Yb^{3+}, Er^{3+} co-doped Y_2O_3 powder was fluorinated by firing the mixed oxide powder and NH_4HF_2 (purity of 99.9%) in a closed corundum crucible at 200°C and 600°C for 3 h, respectively. The fluorinated powder was washed with distilled water to remove residual NH_4HF_2 or NH_4F. After being dried at 80°C for several hours, the final product was obtained. By this method, a series of $Y_{0.97-x}Er_{0.03}Yb_xF_3$ ($x = 0, 0.05, 0.10, 0.15, 0.20$) powders were prepared.

The emission spectra were measured at room temperature by a FLS920 spectrofluorometer equipped with a 450 W Xenon lamp as excitation. All the samples for the spectral measurement were pressed into thin flat disks with the same size ($D = 0.5$ cm) and the surfaces were smoothed, ensuring the condition for the measurement were identical.

Under 365 nm excitation, Fig. 1 presents the emission spectra of the $Y_{0.97-x}Er_{0.03}Yb_xF_3$ samples with $x = 0$ and 0.10. A green emission at 550 nm and a red emission at 650 nm in the visible region are both observed in the two samples. They are ascribed to the $^4S_{3/2} \rightarrow {}^4I_{15/2}$ and $^4F_{9/2} \rightarrow {}^4I_{15/2}$ transitions of Er^{3+}, respectively. With the introduction of Yb^{3+} ions, interestingly, it is found that the green emission decreases, while the red emission increases. The intensity ratio of the red emission to the green one (R) is calculated to be 0.12 at $x = 0$ and 1.14 at $x = 0.10$. At $x = 0$, a weak near infrared emission at 980 nm is also observed, corresponding to the transition $^4I_{11/2} \rightarrow {}^4I_{15/2}$ of Er^{3+}. However, the near infrared emission is obviously broadened and enhanced by the introduction of Yb^{3+} ions, showing that the transition $^2F_{5/2} \rightarrow {}^2F_{7/2}$ of Yb^{3+} ion also contributes to the emission. This indicates that an energy transfer on the combination of Er^{3+} and Yb^{3+} ions performs the QC. As a result, both the red and near infrared emissions are intensified.

To further explore the QC mechanism, the luminescence spectra for the samples with different Yb^{3+} concentrations

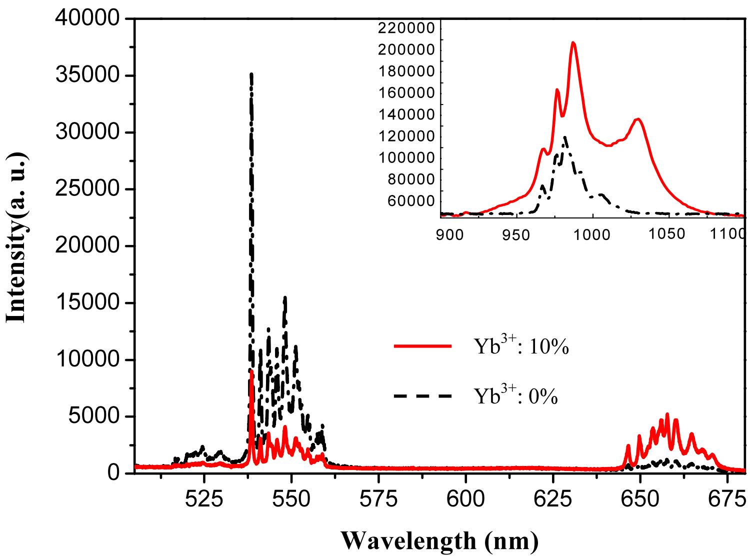

Fig. 1 Emission spectra of Er^{3+}/Yb^{3+} co-doped YF_3 powder with Yb^{3+} concentration of 0% and 10% under the excitation of 365 nm

are all measured excited by both 365 and 488 nm. Figure 2 gives the dependence of the intensity ratio R (R') on Yb^{3+} concentration under 365 nm (488 nm) excitation. It is found that with Yb^{3+} concentration increasing, the intensity ratio R under 365 nm excitation is remarkably increased, while the intensity ratio R' under 488 nm excitation is almost constant.

Based on the luminescence properties, the photon conversion mechanisms under 365 and 488 nm excitations have been respectively proposed, as, shown in Fig. 3. Under the 488 nm excitation, it is found in Fig. 2 that the Yb^{3+} introduction has no influence on the intensity ratio of the red emission to the green one. This means that no energy transfer takes place between the Er^{3+} and Yb^{3+} ions, and the populations of the $^4S_{32}$ and $^4F_{92}$ states are performed by multistep phonon relaxation of Er^{3+}. As a result, the intensity ratio of the red emission to the green one is invariable as a function of Yb^{3+} concentration. Under the 365 nm excitation, the intensified red emission and weakened green emission with the increase of the Yb^{3+} concentration indicates that a cross-relaxation energy transfer enhances the $^4F_{9/2}$ state population and decreases the $^4S_{32}$ state population. Considering the energy matching condition, the possible resonant processes are $^4G_{11/2}(Er^{3+}) + {}^2F_{7/2}(Yb^{3+}) \rightarrow {}^4F_{92}(Er^{3+}) + {}^2F_{5/2}(Yb^{3+})$ and $^2H_{11/2}(Er^{3+}) + {}^2F_{7/2}(Yb^{3+}) \rightarrow {}^4I_{11/2}(Er^{3+}) + {}^2F_{5/2}(Yb^{3+})$. As mentioned above, the Yb^{3+} introduction has no influence on the intensity ratio of the red emission to the green one under the 488 nm excitation. This shows that the probability of the $^2H_{11/2}(Er^{3+}) + {}^2F_{7/2}(Yb^{3+}) \rightarrow {}^4I_{11/2}(Er^{3+}) + {}^2F_{5/2}(Yb^{3+})$ energy transfer is small enough and can be completely neglected even though the energy match condition is satisfied. Therefore, this energy transfer will not take place although the $^2H_{11/2}$ level is also populated by multistep phonon relaxation after the $^4G_{11/2}$ level is excited by 365 nm photons. Thus the only possible energy transfer process is $^4G_{11/2}(Er^{3+}) + {}^2F_{7/2}(Yb^{3+}) \rightarrow {}^4F_{92}(Er^{3+}) + {}^2F_{5/2}(Yb^{3+})$. This process populates the $^4F_{9/2}$ state of Er^{3+}, increasing the red emission. In the meantime,

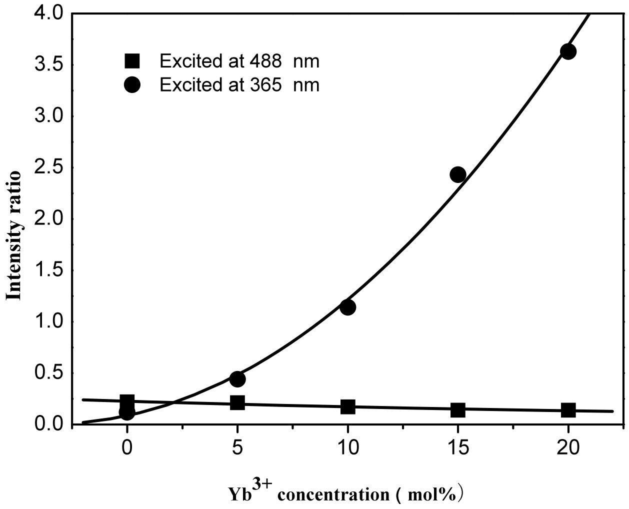

Fig. 2 Intensity ratio of the red emission (650 nm) to the green one (550 nm) excited at 365 nm (*dot*)and 488 nm (*square*)

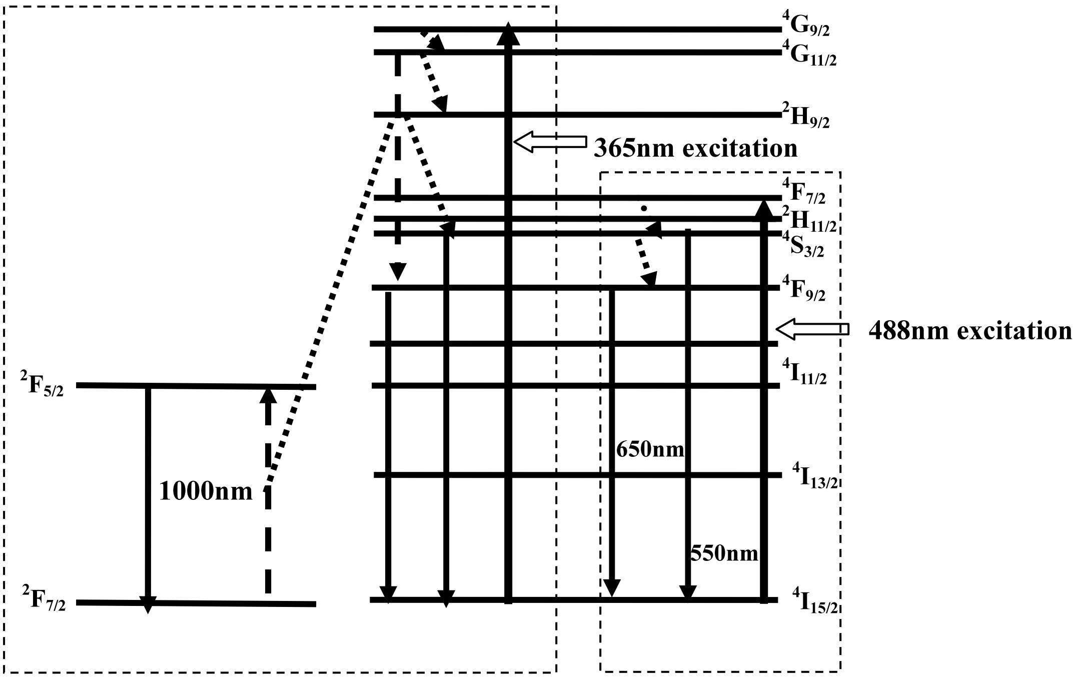

Fig. 3 Photon conversion mechanism under the 488 and 365 nm excitations

it also performs the population of the $^2F_{5/2}$ state of Yb^{3+}, leading to the increased and broadened near infrared emission at 1000 nm. Obviously, the red and near infrared QC down-conversion occurs under the 365 nm excitation, induced by the cross-relaxation energy transfer. This down-conversion is different from previously reported cooperative down-conversion. More interestingly, both the enhanced red and near infrared emissions just fall in the responding region of crystalline Si solar cells and thus are potentially useful to enhance the efficiency of Si-based solar cells.

By comparing the intensity ratios of the green emission to the red one under the 365 and 488 nm excitations, we can estimate the energy transfer efficiency for QC. Under the 488 nm excitation, the intensity ratio R' is expressed as

$$R' = k\xi h r_R A_R/(1-\xi) h r_G A_G, \tag{1}$$

where $r_R (r_G)$ is the frequency of the red (green) emission of Er^{3+}, A_R (A_G) is the radiative rate of the $^4F_{9/2}$ ($^4S_{3/2}$) level of Er^{3+}, h is Planck constant, k is a constant determined by the difference of the responsibility of the detection system for the green and red emission, ξ is the ratio of the particles that is transferred from the $^4S_{3/2}$ state to the $^4F_{9/2}$ state.

Under the 365 nm excitation, neglecting the luminescence emission between the $^4G_{11/2}$ and $^2H_{11/2}$ levels, the intensity ratio R can be expressed as

$$R = k[\eta + (1-\eta)\xi] h r_R A_R/(1-\eta)(1-\xi) h r_G A_G, \tag{2}$$

where η is the energy transfer efficiency for QC. Combining (1) and (2), R/R' is then written as

$$R/R' = \eta + (1-\eta)\xi/(1-\eta)\xi. \tag{3}$$

Assuming that only the multi-phonon relaxation leads to the particles at $^4S_{3/2}$ state relax to the $^4F_{9/2}$ state, ξ can expressed as

$$\xi = W_{nG}/A_G, \tag{4}$$

where W_{nG} is the rate of the multi-phonon relaxation from $^4S_{3/2}$ to $^4F_{9/2}$. W_{nG} and A_G can be adopted as 27.5 and 662 s^{-1}, respectively, which were obtained by Weber [18] for LaF_3. Thus the value of ξ is calculated to be 0.04 in terms of (4). On the other hand, the ratio R/R' has been calculated, as shown in Fig. 2. Hence the energy transfer efficiency η for the QC can be calculated according to (3) for different Yb^{3+} concentrations. The calculated results are shown in Fig. 4. It is found that the energy transfer efficiency for QC increases upon raising Yb^{3+} concentration. At $x = 0.20$, η reaches 50.2%. However, higher Yb^{3+} concentration will result in the quenching of the $^2F_{5/2} \rightarrow {}^2F_{72}$ infrared emission of Yb^{3+}, due to the energy transfers such as $^2F_{5/2}(Yb^{3+}) + {}^4I_{15/2}(Er^{3+}) \rightarrow {}^4I_{11/2}(Er^{3+}) + {}^2F_{7/2}(Yb^{3+})$. Figure 5 shows the infrared emission in the range of 900–110 nm as a function of Yb^{3+} concentration, the infrared emission tends to decrease when the Yb^{3+} concentration is higher than 10% (mol). This means that the total down-converted emission will decrease at higher Yb^{3+} content due to the concentration quenching, although the energy transfer efficiency for QC is enhanced.

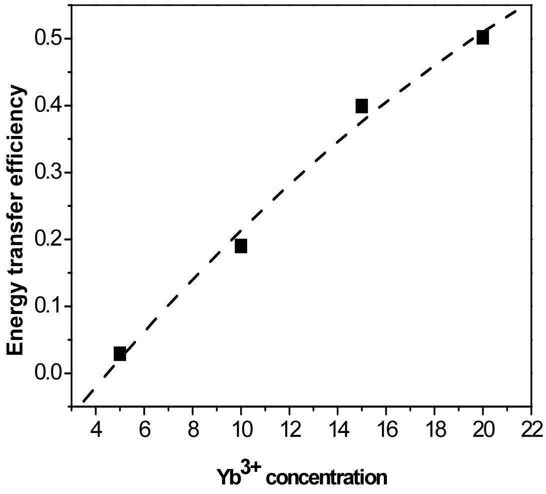

Fig. 4 Energy transfer efficiency for QC as a function of Yb^{3+} concentration

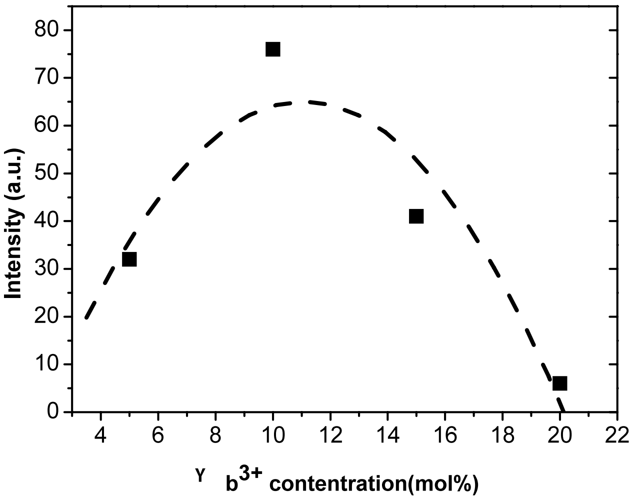

Fig. 5 Infrared emission intensity as a function of Yb^{3+} concentration

In summary, an energy transfer induced red and near infrared down-conversion pumped with 365 nm has been achieved in Er^{3+}/Yb^{3+} co-doped YF_3 powder, which is different from the traditional cooperative down-conversion. Both of the produced photons fall in the responding region of widely used Si-based solar cells. The energy transfer efficiency for QC is estimated by comparing the intensity ratios of the green emission to the red one under the 365 and 488 nm excitations. It is shown that the Er^{3+}/Yb^{3+} co-doped YF_3 have potential applications for Si-based solar cells of high energy efficiency by down-converting the high energy part of the solar spectrum.

Acknowledgements This work is supported by National Natural Science Foundation of China (No. 10674113 and 10847103), Program for New Century Excellent Talents in University (NCET-06-0707), Foundation for the Author of National Excellent Doctoral Dissertation of China (Grant No. 200726).

References

1. J.L. Sommerdijk, A. Bril, A.W. de Jager, J. Lumin. **8**, 341 (1974)
2. W.W. Piper, J.A. DeLuca, F.S. Ham, J. Lumin. **8**, 344 (1974)
3. R. Pappalardo, J. Lumin. **14**, 159 (1976)
4. R.T. Wegh, H. Donker, A. Meijerink, R.J. Lamminmäki, J. Hölsä, Phys. Rev. B **56**, 13841 (1997)
5. R.T. Wegh, H. Donker, K.D. Oskam, A. Meijerink, Science **283**, 663 (1999)
6. R.T. Wegh, E.V.D. van Loef, A. Meijerink, J. Lumin. **90**, 111 (2000)
7. T.J. Lee, L.Y. Luo, W.G. Diau, T.M. Chen, B.M. Cheng, C.Y. Tung, Appl. Phys. Lett. **89**, 131121 (2006)
8. Y.H. Chen, C.S. Shi, W.Z. Yan, Z.M. Qi, Y.B. Fu, Appl. Phys. Lett. **88**, 061906 (2006)
9. Z.G. Nie, J.H. Zhang, X. Zhang, S.Z. Lu, X.G. Ren, G.B. Zhang, X.J. Wang, Solid State Chem. **180**, 2933 (2007)
10. K.D. Oskam, R.T. Wegh, H. Donker, E.V.D. van Loef, A. Meijerink, J. Alloys Compd. **300–301**, 421 (2000)
11. P. Vergeer, T.J.H. Vlugt, M.H.F. Kox, M.I. den Hertog, J.P.J.M. van der Eerden, A. Meijerink, Phys. Rev. B **71**, 014119 (2005)
12. Q.Y. Zhang, G.F. Yang, Z.H. Jiang, Appl. Phys. Lett. **91**, 051903 (2007)
13. L. Xie, Y. Wang, H. Zhang, Appl. Phys. Lett. **94**, 061905 (2009)
14. D. Chen, Y. Wang, Y. Yu, P. Huang, F. Weng, J. Appl. Phys. **104**, 116105 (2008)
15. J.F. Suyver, A. Aebischer, D. Biner, P. Gerner, J. Grimm, S. Heer, K.W. Krämer, C. Reinhard, H.U. Güdel, Opt. Mater. **27**, 1111 (2005)
16. R.C. Powell, *Physics of Solid-State Laser Materials* (Springer, New York, 1998)
17. S. Xiao, X. Yang, J.W. Ding, X.H. Yan, J. Phys. Chem. C **111**, 8161 (2007)
18. M.J. Weber, Phys. Rev. **157**, 262 (1967)